

FINAL CONTRACT REPORT

**DEVELOPMENT OF CONCRETE SHRINKAGE
PERFORMANCE SPECIFICATIONS**

David W. Mokarem, Ph.D.
Research Scientist
Virginia Transportation Research Council

Richard M. Meyerson
Bridge Engineer
Reynolds, Smith and Hills

Richard E. Weyers, Ph.D., P.E.
Professor
Department of Civil and Environmental Engineering
Virginia Polytechnic Institute and State University

Project Manager

D. Stephen Lane, Virginia Transportation Research Council

Contract Research Sponsored by
The Virginia Transportation Research Council

Virginia Transportation Research Council
(A Cooperative Organization Sponsored Jointly by the
Virginia Department of Transportation and
the University of Virginia)

Charlottesville, Virginia

August 2003
VTRC 04-CR1

NOTICE

The project that is the subject of this report was done under contract for the Virginia Department of Transportation, Virginia Transportation Research Council. The contents of this report reflect the views of the authors, who are responsible for the facts and the accuracy of the data presented herein. The contents do not necessarily reflect the official views or policies of the Virginia Department of Transportation, the Commonwealth Transportation Board, or the Federal Highway Administration. This report does not constitute a standard, specification, or regulation.

Each contract report is peer reviewed and accepted for publication by Research Council staff with expertise in related technical areas. Final editing and proofreading of the report are performed by the contractor.

Copyright 2003 by the Commonwealth of Virginia.

ABSTRACT

During its service life, concrete undergoes volume changes. One of the types of deformation is shrinkage. The four main types of shrinkage associated with concrete are plastic, autogenous, carbonation, and drying shrinkage. The volume changes in concrete due to shrinkage can lead to the cracking of the concrete. In the case of reinforced concrete, the cracking may produce a direct path for chloride ions to reach the reinforcing steel. Once chloride ions reach the steel surface, the steel will corrode, which itself can cause cracking, spalling, and delamination of the concrete.

The unrestrained drying shrinkage and restrained cracking tendency of concrete mixtures typically used by the Virginia Department of Transportation (VDOT) were assessed to establish an appropriate limit on drying shrinkage for use in a performance specification. Five existing shrinkage prediction models were assessed to determine the accuracy and precision of each model as it pertains to the VDOT mixtures used in this study. The five models assessed were the ACI 209 Code Model, Bazant B3 Model, CEB 90 Code Model, Gardner/Lockman Model, and Sakata Model. The CEB 90 model performed best for the portland cement concrete mixtures, while the Gardner/Lockman Model performed best for the supplemental cementitious material mixtures.

Based on a comparison of the unrestrained drying shrinkage and restrained cracking tendency, it was determined that the potential for cracking could be minimized by limiting the unrestrained shrinkage of the concrete mixtures. Based on the results of this study, the recommended percentage length change specification limits are 0.0300 at 28 days and 0.0400 at 90 days for the portland cement concrete mixtures. For the supplemental cementitious material mixtures, the percentage length change specification limits were 0.0400 at 28 days and 0.0500 at 90 days.

FINAL CONTRACT REPORT

DEVELOPMENT OF CONCRETE SHRINKAGE PERFORMANCE SPECIFICATIONS

David W. Mokarem, Ph.D.
Research Scientist
Virginia Transportation Research Council

Richard M. Meyerson
Bridge Engineer
Reynolds, Smith and Hills

Richard E. Weyers, Ph.D., P.E.
Professor
Department of Civil and Environmental Engineering
Virginia Polytechnic Institute and State University

INTRODUCTION

Volume changes in concrete due to autogenous shrinkage and moisture loss can result in the early deterioration of reinforced concrete. As concrete cures and dries, tensile stresses are created due to the concrete's resistance to volume changes. Drying shrinkage is defined as the decrease in concrete volume with time due to moisture loss, whereas autogenous shrinkage is defined as the reduction in volume of the concrete due to hydration of the cement. Drying shrinkage cracking is related not only to the amount of shrinkage, but also to the modulus of elasticity, creep, and tensile strength of the concrete (Mehta and Monteiro, 1993).

In the case of reinforced concrete, the cracking of the concrete due to the combination of drying and autogenous shrinkage may lead to corrosion of the reinforcing steel. Chloride ions, which are present in seawater and deicer salts, reach the steel surface either by diffusion through the concrete pore water or through cracks in the concrete. Once chloride ions reach the steel surface, the steel will corrode; the corrosion products can cause cracking, spalling, and delamination of the concrete. In the case of prestress concrete systems, drying shrinkage is an important factor. The strain produced in the concrete from drying shrinkage leads to a reduction of strain in the prestressed steel. This in turn contributes to prestress losses in the system.

Much of the current research stresses the development of low-permeability concretes to reduce the effects of corrosion and other deterioration mechanisms. However, little research has been directed toward the reduction of cracking in concrete. The development of low-permeability concrete with a reduced propensity for cracking will help to reduce the deterioration of reinforced concrete from the ingress of aggressive ions through cracks.

There are cost savings associated with the reduction of shrinkage cracking in concrete bridge decks and superstructures. The cost of a new deck with epoxy coated rebar (ECR) is

\$13.35 per square foot (Brown, 2002). It is estimated that about 1 million square feet of deck are constructed per year, for a total cost of \$13.35 million per year. If there are no cracks from shrinkage, the deck design life is 75 years. However, if there is cracking, the deck needs an overlay in 50 years at a cost of \$12.03 per square foot. The use of an overlay creates a cost of \$25.38 million per year. Therefore, without a shrinkage specification, the cost would be \$25.38 million per year as opposed to \$13.35 million per year. If the shrinkage specification keeps the cracks to a minimum, the savings could be around \$12.03 million per year.

BACKGROUND

Concrete experiences volume changes throughout its service life. The total in-service volume change is the resultant of applied loads, shrinkage, and contraction. When loaded, concrete experiences an instantaneous recoverable elastic deformation and a slow inelastic deformation called creep. Creep of concrete is composed of two components: basic creep, or deformation under constant load without moisture loss or gain, and drying creep. Drying creep is the time-dependent deformation of a drying specimen under constant load minus the sum of the drying shrinkage and basic creep. Deformation of concrete in the absence of applied loads is often called shrinkage. There are four main types of shrinkage. The shrinkage mechanisms in concrete shall be addressed and include a theoretical and empirical background.

Shrinkage Mechanism

There are four main types of shrinkage in concrete: plastic, autogeneous, carbonation, and drying shrinkage. Plastic shrinkage is due to moisture loss from the concrete before the concrete sets. Autogeneous shrinkage is associated with the loss of water from the capillary pores due to the hydration of the cement (Holt and Janssen, 1998). This type of shrinkage tends to increase at higher temperatures and at higher cement contents. In general, it is relatively small and is not distinguished from shrinkage caused by drying of concrete. Carbonation shrinkage is caused by the chemical reaction of various cement hydration products with carbon dioxide present in the air. This type of shrinkage is usually limited to the surface of the concrete (Dilger and Wang, 1997). Drying shrinkage can be defined as the volumetric change due to drying of the concrete.

Theoretical

Numerous papers have discussed the mechanisms that affect drying shrinkage in concrete. Capillary depression, variations in surface tension, and variations in disjoining pressure are all associated with the movement and loss of water from concrete during drying (Hau et al., 1995, Hansen, 1987a). The variation of capillary depression is deduced from the Laplace and Kelvin laws:

$$p_v - p_c = \frac{2\sigma}{r} \cos \theta \quad (\text{Laplace})$$

$$p_c - p_v = \frac{RT}{Mv} \ln(H) \quad (\text{Kelvin})$$

where: σ = surface tension of water/water vapor interface
 θ = moistening angle
 p_c = pressure in water
 p_v = pressure in water vapor
 r = radius of pore where there is a meniscus
 v = specific volume of water
 M = molar mass of water
 R = ideal gas constant
 T = temperature
 H = relative humidity

Hau et al. (1995) discussed that in a given unsaturated state, there exists an access radius, r . All capillaries with a radius less than the access radius are filled with water, and all capillaries with a radius greater than the access radius are empty. This introduces a corresponding tension in the liquid phase, thus; the solid skeleton undergoes compression.

The mechanism of surface tension deals with the attractive forces of atoms or molecules at the surface. This mechanism operates at low relative humidities. Above a certain relative humidity, the entire surface is covered by adsorbed water molecules; thus, the variation in relative humidity can no longer vary the surface tension.

The mechanism of disjoining pressure concerns the interaction between two solid surfaces. As the thickness of the adsorbed water molecule layer increases, it can no longer develop freely. As the relative humidity increases, the adsorption of water tends to separate the two solid surfaces. Thus, the two surfaces undergo a pressure called “disjoining pressure.” The maximum disjoining pressure occurs at the saturated state. When the system goes from a saturated to an unsaturated state, shrinkage occurs because of decreased disjoining pressure.

Empirical

Neville (1998) discussed the loss of water in concrete associated with drying shrinkage. The change in volume of the concrete is not equal to the volume of the water lost. The loss of free water occurs first; this causes little to no shrinkage. As the drying of the concrete continues, the adsorbed water is removed. This adsorbed water is held by hydrostatic tension in small capillaries (< 50 nm). The loss of this water produces hydrostatic tensile stresses, which induce compressive stresses on the rigid skeleton causing the concrete to shrink. The shrinkage due to this water loss is significantly greater than that associated with the volume of free water lost (Mindess & Young, 1981).

DeLarrard et al. (1994) discussed some of the factors that affect the magnitude of drying shrinkage in concrete. These factors include the aggregate used, the water/cement ratio (w/c), the relative humidity, and the member size. The aggregate used in the concrete mixture acts to restrain the shrinkage of the cement paste. Concrete with a higher aggregate content has less shrinkage than those with a lower aggregate content. Aggregates with a higher modulus of elasticity or a rougher surface are more resistant to shrinkage. In general, a higher w/c ratio will

produce greater drying shrinkage (Hansen, 1987a). With a higher w/c ratio, the strength and stiffness of the paste are decreased, which can lead to increased shrinkage. As with creep, there is a lower shrinkage at higher relative humidities. Member size also plays a role in drying shrinkage: the greater the volume to surface area ratio of the member, the less the drying shrinkage.

Reversible drying shrinkage is the part of the drying shrinkage of the concrete that is reproducible during wetting and drying cycles (Mehta and Monteiro, 1993). Irreversible drying shrinkage is the part of the total drying shrinkage during the first drying cycle that cannot be reproduced during subsequent wetting and drying cycles. The authors state that the irreversible shrinkage is probably due to the development of chemical bonds within the calcium silicate hydrate structure as a consequence of drying of the concrete.

Drying shrinkage can cause cracking in concrete. The cracking is due to tensile stresses caused by the restraint conditions. Thus, drying shrinkage is related to not only the amount of shrinkage but also the modulus of elasticity, creep, and tensile strength of the concrete (Suzuki et al., 1993). All of these properties vary with time, so it is difficult to determine the cracking tendency of the concrete based solely on shrinkage. Therefore, the modeling of creep and shrinkage of concrete has to take into account many different variables.

PURPOSE AND SCOPE

The objective of this study was two-fold. The first objective was to develop a concrete shrinkage performance specification and an associated test procedure. The test procedure can then be used to measure and place limits for the amount of drying shrinkage in concrete mixtures purchased by the Virginia Department of Transportation (VDOT).

The second objective was to assess the accuracy of existing unrestrained shrinkage prediction models for a range of typical VDOT mixtures.

The proposed study was limited to A3–General Paving (3000 psi at 28 days), A4–General Bridge Deck (4000 psi at 28 days), and A5–General Prestress (5000 psi at 28 days) concrete mixtures approved by the VDOT. Some of these mixtures included slag cement, and some included pozzolans such as fly ash and microsilica. In addition, three types of normal weight coarse aggregate, limestone, gravel, and diabase, and their associated fine aggregate were included as variables. Chemical admixtures such as air entrainers, retarders, and high-range water reducers were also included in the mixtures. However, the chemical admixtures were not a study variable, as only one type and one manufacturer of each admixture were used.

METHODS AND MATERIALS

Restrained Shrinkage Testing

The restrained shrinkage testing was conducted in accordance with AASHTO PP34-98, Standard Practice for Estimating the Cracking Tendency of Concrete (AASHTO, 1998). The test

method involves casting a concrete ring around a steel ring. Sonotube was used as a form for casting the concrete around the steel ring. Figure 1 presents the specimen configuration. Strain gages were mounted on the inside of the steel ring to monitor the strain in the steel ring caused by the shrinkage of the concrete.

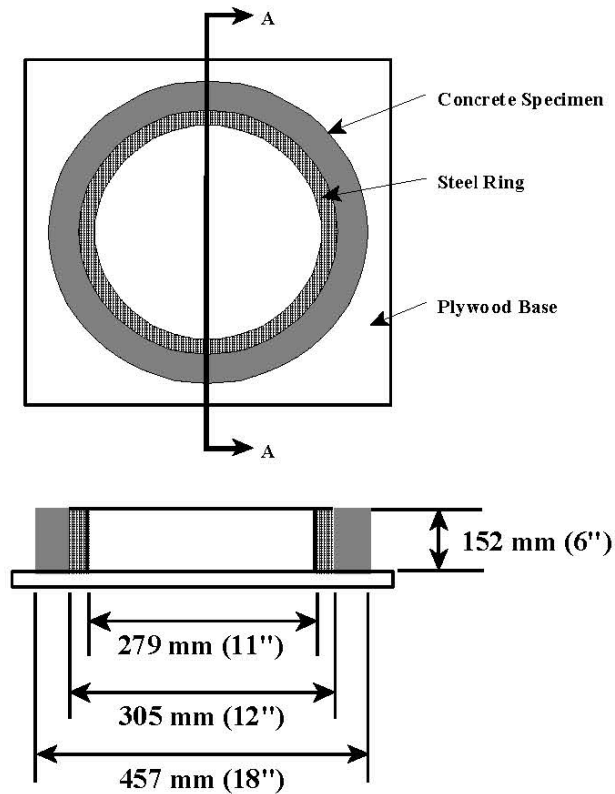


Figure 1. Restrained Shrinkage Specimen Configuration

As the concrete shrinks, a compressive stress is produced in the steel ring, which is balanced by a tensile stress in the concrete. When cracking occurs in the concrete, the stress and thus the strain in the steel ring are released.

The specimens were cured and measured in the following manner. Immediately after the specimens were fabricated, an initial strain measurement was conducted. Each strain gage was measured using a strain indicator. The specimens were then placed in a controlled environment of $23\text{ }^{\circ}\text{C} \pm 2\text{ }^{\circ}\text{C}$ and $50\% \pm 4\%$ relative humidity. The specimens were then covered with wet burlap and a 0.15-mm polyethylene sheet and allowed to cure for 24 hours. After 24 hours, the sonotube molding was removed. A 0.15-mm polyethylene sheet was then adhered to the top surface of the concrete ring. This was done to limit the drying of the concrete from only the annular exposed face. Strain measurements were then taken on each strain gage. Strain readings were taken again at 7 days, then every 7 days until 90 days. Subsequent readings were taken at 120, 150, and 180 days.

The specimens were visually monitored on a daily basis for cracking. Cracking became visible when the crack width was approximately 0.2 mm (0.008 in). Strain readings were also monitored to detect cracking. After cracking occurred, strain readings were taken on all strain gages on a daily basis for 14 days. The crack width and length were also measured on a daily basis for the 14 days after cracking occurred. The crack width was measured at three locations along the crack length, and an average was calculated.

Unrestrained Shrinkage Testing

Unrestrained shrinkage testing was conducted in accordance with ASTM C 157-98, Standard Test Method for Length Change of Hardened Hydraulic-Cement Mortar and Concrete (ASTM,1998). The test method involves measuring the length change of 75 mm x 75 mm x 279 mm (3 in x 3 in x 11 ¼ in) concrete prisms.

Specimens were fabricated in steel molds according to ASTM C 192-98, Practice for Making and Curing Concrete Test Specimens in the Laboratory. The specimens were then covered with wet burlap and a 0.15-mm polyethylene sheet for 24 hours. After 24 hours of wet curing, the specimens were removed from the steel molds. Initial measurements using a comparator were then taken on each specimen in accordance with ASTM C 490-98, Practice for Use of Apparatus for the Determination of Length Change of Hardened Cement Paste, Mortar, and Concrete. After initial readings were taken, the specimens were placed in lime-saturated water at 23 °C ± 1°C. The specimens were kept in the lime-saturated water for a period of 6 days, with length change measurements being conducted each day. After 6 days in lime-saturated water, the specimens were removed and placed in a controlled environment of 23 °C ± 2 °C and 50% ± 4% relative humidity. Subsequent length change measurements were conducted every 7 days up to 90 days, and then at 120, 150, and 180 days.

Compressive Strength Testing

Compressive strength specimens were fabricated for each concrete mixture in accordance with ASTM C 192-98. Cylindrical specimens were fabricated for testing at seven, 28, 56, and 90 days. The specimen dimensions were 102 mm x 203 mm (4 in x 8 in). Specimens were tested in accordance with ASTM C 39-98, Test Method for Compressive Strength of Cylindrical Concrete Specimens.

Modulus of Elasticity Testing

Modulus of elasticity specimens were fabricated for each concrete mixture in accordance with ASTM C 192-98. Cylindrical specimens were fabricated for testing at 7, 28, 56, and 90 days. The specimen dimensions were 152 mm x 305 mm (6 in x 12 in). Specimens were tested in accordance with ASTM C 469-98, Test Method for Static Modulus of Elasticity and Poisson's Ratio of Concrete in Compression.

Aggregate Properties

Three types of No. 57 coarse aggregate were used for this study: limestone, gravel, and diabase. Coarse along with the fine aggregates commonly used with the particular coarse aggregate were obtained from various locations in Virginia. Samples were taken from each aggregate source in accordance with ASTM D 75-98, Practice for Sampling Aggregates. A sieve analysis was performed on each aggregate sample in accordance with ASTM C 136-98, Method for Sieve Analysis of Fine and Coarse Aggregates. All of the aggregate met VDOT's Required specifications (VDOT, 1997). Specific gravity and absorption tests were conducted in accordance with ASTM C 127-98, Test Method for Specific Gravity and Absorption of Coarse Aggregate, and ASTM C 128-98, Test Method for Specific Gravity and Absorption of Fine Aggregate. The aggregate properties are presented elsewhere (Mokarem, 2002).

Cement Properties

The portland cement used in this study was a Type I/II that met ASTM C 150-98, Specification for Portland Cement. Type I is classified as normal cement, and Type II is classified as moderate sulfate resistance. For this study a blend of Type I/II portland cement and 40% (by weight) ground granulated blast furnace slag (GGBFS) was also used for select mixtures. The GGBFS was grade 120 and met ASTM C 989-98, Specification for Ground Granulated Blast-Furnace Slag for Use in Concrete and Mortars.

Pozzolans

The pozzolans used in this study were Class F fly ash and microsilica, which is a relatively pure amorphous silica that is 100 times finer than portland cement. Both pozzolans were tested according to ASTM C 311-97. The fly ash met ASTM C 618-97 specifications and the microsilica met ASTM C 1240-97 specifications.

Mixture Test Series

Mixtures for this study consisted of A3, A4, and A5 mixtures using portland cement as the binder. Mixtures consisting of portland cement and various supplemental cementitious materials as the binder were also tested. Tables 1 through 3 present the mixture proportions for A3, A4, and A5 mixtures using portland cement as the binder. Table 4 presents the mixture proportions for mixtures using supplemental cementitious materials as the binder. The tables also present the chemical admixture dosages, air-entrainment (AEA), retarder, and high-range water reducer (HRWR) used in the various mixtures.

Table 1. A3 Portland Cement Concrete Mixtures

Ingredient	Limestone		Gravel		Diabase	
	kg/m ³	lb/yd ³	kg/m ³	lb/yd ³	kg/m ³	lb/yd ³
Cement	349	588	335	564	349	588
Fine Agg.	810	1365	685	1154	716	1207
Coarse Agg.	1029	1734	1098	1850	1138	1918
Water	171	289	154	259	166	279
Total	2359	3976	2271	3827	2368	3992
AEA, mL		131		125		131
HRWR, mL		1740		1669		1740
w/c		0.49		0.46		0.47

Table 2. A4 Portland Cement Concrete Mixtures

Ingredient	Limestone		Gravel		Diabase	
	kg/m ³	lb/yd ³	kg/m ³	lb/yd ³	kg/m ³	lb/yd ³
Cement	377	635	377	636	377	636
Fine Agg.	763	1286	584	984	667	1125
Coarse Agg.	1029	1734	1098	1850	1138	1918
Water	170	286	158	267	163	275
Total	2338	3941	2217	3737	2346	3954
AEA, mL		141		141		141
HRWR, mL		1880		1880		1880
Retard. mL		564		564		564
w/c		0.45		0.42		0.43

Table 3. A5 Portland Cement Concrete Mixtures

Ingredient	Limestone		Gravel		Diabase	
	kg/m ³	lb/yd ³	kg/m ³	lb/yd ³	kg/m ³	lb/yd ³
Cement	415	700	418	705	419	706
Fine Agg.	781	1316	640	1078	670	1130
Coarse Agg.	1043	1758	1098	1850	1138	1918
Water	138	233	148	250	164	276
Total	2377	4007	2304	3883	2391	4030
AEA, mL		155		157		157
HRWR, mL		2072		2087		2090
w/c		0.33		0.35		0.39

Table 4. Supplemental Cementitious Materials Mixtures

Ingredient	A4 – Fly Ash		A4 - Microsilica		A4 – Slag Cement		A5 – Slag Cement	
	kg/m ³	lb/yd ³	kg/m ³	lb/yd ³	kg/m ³	lb/yd ³	kg/m ³	lb/yd ³
Cement	321	541	351	591	227	382	252	424
SCM	75	127	27	45	151	254	167	282
Fine Agg.	641	1081	669	1128	667	1125	670	1130
Coarse Ag.	1138	1918	1138	1918	1138	1918	1138	1918
Water	163	275	163	275	163	275	164	276
Total	2339	3942	2348	3957	2346	3954	2391	4030
AEA, mL		148		141		141		157
HRWR, mL		1977		1883		1883		2090
Retard. mL		692		659		659		0
w/c+p		0.43		0.43		0.43		0.39

Specimens were fabricated and tested in three series. The first series consisted of A3, A4, and A5 mixtures for all three coarse aggregates, using portland cement as the binder. Table 5 presents the specimens fabricated for test series 1. The second series consisted of three A4 and an A5 mixture using diabase as the coarse aggregate. The three A4 mixtures included either fly ash, microsilica, or slag cement with portland cement as the binder. The A5 mixture included slag cement and portland cement as the binder. The pozzolans and slag cement were proportioned on a weight basis in the mixtures according to VDOT-approved mixtures as follows:

- Fly ash: remove 15% portland cement, replace with 20% fly ash
- Microsilica: replace 7% portland cement with 7% microsilica
- Slag Cement: replace 40% portland cement with 40% slag cement

Table 6 presents the specimens fabricated for test series 2. The third series consisted of A3, A4, and A5 mixtures for all three coarse aggregates, using portland cement as the binder. Table 7 presents the specimens fabricated for test series 3.

Table 5. Test Series 1 Specimen Fabrication Per Batch

Mixture	Batches	Rings	Prisms	4x8 Cylinders	6x12 Cyl.
A3-Limestone	1	2	2	8	1
A3-Gravel	1	2	2	8	1
A3-Diabase	1	2	2	8	1
A4-Limestone	1	2	2	8	1
A4-Gravel	1	2	2	8	1
A4-Diabase	1	2	2	8	1
A5-Limestone	1	2	2	8	1
A5-Gravel	1	2	2	8	1
A5-Diabase	1	2	2	8	1

Table 6. Test Series 2 Specimen Fabrication Per Batch

Mixture	Batches	Rings	Prisms	4x8 Cylinders	6x12 Cyl.
A4-D/FA	3	2	6	8	1
A4-D/Microsilica	3	2	6	8	1
A4-D/Slag	3	2	6	8	1
A5-D/Slag	3	2	6	8	1

Table 7. Test Series 3 Specimen Fabrication Per Batch

Mixture	Batches	Rings	Prisms	4x8 Cylinders	6x12 Cyl.
A3-Limestone	3	0	3	8	1
A3-Gravel	3	0	3	8	1
A3-Diabase	3	0	3	8	1
A4-Limestone	3	0	3	8	1
A4-Gravel	3	0	3	8	1
A4-Diabase	3	0	3	8	1
A5-Limestone	3	0	3	8	1
A5-Gravel	3	0	3	8	1
A5-Diabase	3	0	3	8	1

Existing Prediction Models

Five existing shrinkage prediction models were used to compare the actual shrinkage measurements obtained in this study to the predicted values of each model. The following presents the equations for the five existing prediction models:

American Concrete Institute – ACI 209 Code Model (Bhal and Jain, 1996, Mehta and Monteiro, 1986)

$$\varepsilon_{sh}(t, t_{sh,o}) = \frac{(t - t_{sh,o})}{35 + (t - t_{sh,o})} \varepsilon_{sh\infty} \text{ (moist / cure)}$$

$$\varepsilon_{sh}(t, t_{sh,o}) = \frac{(t - t_{sh,o})}{55 + (t - t_{sh,o})} \varepsilon_{sh\infty} \text{ (steam / cure)}$$

where: $\varepsilon_{sh}(t, t_{sh,o})$ = shrinkage strain (in/in)
 t = time (days)
 $t_{sh,o}$ = time at start of drying (days)
 $\varepsilon_{sh\infty}$ = ultimate shrinkage strain (in/in)

Bazant B3 Model (Bazant, 1995)

$$\varepsilon_{sh}(t, t_o) = -\varepsilon_{sh\infty} K_h S(t)$$

$$\varepsilon_{sh\infty} = -\alpha_1 \alpha_2 \left(26(w)^{2.1} (f_c')^{-0.28} + 270 \right) * 10^{-6}$$

$$K_h = 1 - h^3$$

$$S(t) = \tanh \sqrt{\frac{t - t_o}{T_{sh}}}$$

where: $\varepsilon_{sh}(t, t_o)$ = shrinkage strain (in/in)
 $\varepsilon_{sh\infty}$ = ultimate shrinkage strain (in/in)
 w = water content of concrete (lb/ft³)
 K_h = cross-section shape factor
 h = relative humidity (%)

t = age of concrete (days)
 t_0 = age of concrete at beginning of shrinkage
 $S(t)$ = time function for shrinkage

Euro-International Concrete Committee – CEB 90 Code Model
 (Bhal and Jain, 1996, Mehta and Monteiro, 1986)

$$\varepsilon_{cso} = \varepsilon_s(f_{cm})(\beta_{RH})$$

$$\varepsilon_s(f_{cm}) = (160 + 10\beta_{sc}(9 - f_{cm}/1450)) * 10^{-6}$$

$$\beta_{RH} = -1.55\beta_{ARH}$$

$$\beta_{ARH} = 1 - (RH / 100)^3$$

where: ε_{cso} = drying shrinkage of portland cement concrete (in/in)
 ε_s = drying shrinkage obtained from RH-shrinkage chart
 β_{sc} = coefficient depending on type of cement
 β_{RH} = coefficient for relative humidity
 f_{cm} = mean 28-day compressive strength (psi)

Gardner/Lockman Model
 (Gardner and Lockman, 2001)

$$\varepsilon_{sh} = \varepsilon_{shu}\beta(h)\beta(t)$$

$$\varepsilon_{shu} = 1000 * K * \left(\frac{4350}{f_{cm28}} \right)^{1/2} * 10^{-6}$$

$$\beta(h) = 1 - 1.18h^4$$

$$\beta(t) = \left(\frac{(t - t_c)}{t - t_c + 97(V/S)^{1/2}} \right) * 10^{-6}$$

where: ε_{sh} = shrinkage strain (in/in)

ϵ_{shu} = ultimate shrinkage strain (in/in)
 $\beta(h)$ = correction term for effect of humidity on shrinkage
 $\beta(t)$ = correction term for effect of time on shrinkage
 h = humidity
 t_c = age drying commenced (days)
 t = age of concrete (days)
 K = correction term for effect of cement type

Sakata Model

(Sakata, 1993)

$$\epsilon_{sh}(t, t_o) = \epsilon_{sh\infty} \left[1 - \exp\{-0.108(t - t_o)^{0.56}\} \right]$$

$$\epsilon_{sh\infty} = -50 + 78(1 - \exp(RH / 100) + 38(\ln(w)) - 5(\ln(V / S) / 10)^2 * 10^{-5}$$

where: $\epsilon_{sh}(t, t_o)$ = predicted shrinkage strain (in/in)
 $\epsilon_{sh\infty}$ = ultimate shrinkage strain (in/in)
 w = water content of the concrete (kg/m³)
 RH = relative humidity (%)
 V/S = volume-to-surface area ratio
 t = time (days)
 t_o = time drying started (days)

RESULTS

This section presents the results of the standard compressive strength, modulus of elasticity, restrained shrinkage, and unrestrained shrinkage tests. Also presented are the residuals for the five shrinkage prediction models. The compressive strength, modulus of elasticity, and unrestrained shrinkage test results are for the first and third test series of A3, A4, and A5 portland cement concrete mixtures. The second test series involves the supplemental cementitious material mixtures. Restrained shrinkage test specimens were fabricated for test series 1 and 2 only. The compressive strengths, modulus of elasticity, and unrestrained shrinkage test results for test series 1 and 3 were not significantly different. Therefore, the test results were combined to form an A3 test group, A4 test group, and A5 test group.

Compressive Strength

Table 8 presents the average compressive strengths for the mixtures at 7, 28, and 90 days. Two 102 mm x 204 mm (4 in x 8 in) cylinders were tested for each mixture at 7, 28, and 90 days.

Table 8. Average Compressive Strength Test Results

A3-Portland Cement Concrete Mixtures							
	w/c	7 Days		28 Days		90 Days	
		MPa	psi	MPa	psi	MPa	psi
Limestone	0.49	32.9	4770	39.2	5680	45.3	6570
Gravel	0.46	37.1	5380	41.3	5990	47.6	6900
Diabase	0.47	36.7	5330	41.4	6010	47.3	6860
A4-Portland Cement Concrete Mixtures							
	w/c	7 Days		28 Days		90 Days	
		MPa	psi	MPa	psi	MPa	psi
Limestone	0.45	36.3	5260	43.1	6250	47.8	6940
Gravel	0.42	38.1	5530	44.4	6440	50.7	7360
Diabase	0.43	36.7	5330	43.5	6310	48.7	7070
A5-Portland Cement Concrete Mixtures							
	w/c	7 Days		28 Days		90 Days	
		MPa	psi	MPa	psi	MPa	psi
Limestone	0.33	49.3	7150	53.2	7720	58.1	8420
Gravel	0.35	43.2	6260	48.8	7080	55.4	8035
Diabase	0.39	41.9	6070	47.4	6870	52.3	7580
Supplemental Cementitious Material Mixtures							
	w/c+p	7 Days		28 Days		90 Days	
		MPa	psi	MPa	psi	MPa	psi
A4-D/FA	0.43	47.9	6950	53.4	7740	58.1	8430
A4-D/MS	0.43	47.4	6870	52.7	7650	60.1	8720
A4-D/S	0.43	50.2	7280	54.3	7880	61.0	8850
A5-D/S	0.39	51.4	7450	55.3	8020	62.3	9030

Modulus of Elasticity

Table 9 presents the average modulus of elasticity for the mixtures used in this study at 7, 28, and 90 days after casting of the specimens. The test was performed twice at seven, 28, and 90 days, and the modulus of elasticity values in the table represent the average of the two measurements. The table also presents the estimated modulus of elasticity using the AASHTO standard specification (AASHTO, 1996). The AASHTO results were within 10% of the actual measured values. The following equation was used for the AASHTO results:

$$E_c = 0.43\gamma^{1.5} \sqrt{f'_c} \quad (\text{Eq. 1})$$

where:

- E_c = modulus of elasticity (GPa)
- γ = unit weight of concrete (kg/m^3)
- f'_c = average 28-day compressive strength (MPa)

Table 9. Average Modulus of Elasticity Test Results

A3 – Portland Cement Concrete Mixtures								
	7 Days		28 Days		90 Days		AASHTO	
	GPa	x 10⁶psi	GPa	x 10⁶psi	GPa	x 10⁶psi	GPa	x 10⁶psi
Limestone	27.0	3.91	28.8	4.17	31.2	4.52	29.0	4.20
Gravel	27.9	4.05	29.5	4.28	31.6	4.59	29.5	4.28
Diabase	27.9	4.05	29.4	4.27	31.6	4.58	29.4	4.27
A4 – Portland Cement Concrete Mixtures								
	7 Days		28 Days		90 Days		AASHTO	
	GPa	x 10⁶psi	GPa	x 10⁶psi	GPa	x 10⁶psi	GPa	x 10⁶psi
Limestone	27.6	4.01	29.6	4.30	33.7	4.89	31.0	4.49
Gravel	28.8	4.18	30.7	4.45	35.2	5.10	31.1	4.51
Diabase	27.6	4.00	29.9	4.34	34.3	4.97	30.0	4.35
A5 – Portland Cement Concrete Mixtures								
	7 Days		28 Days		90 Days		AASHTO	
	GPa	x 10⁶psi	GPa	x 10⁶psi	GPa	x 10⁶psi	GPa	x 10⁶psi
Limestone	33.2	4.81	35.0	5.08	39.0	5.66	35.6	5.16
Gravel	31.5	4.57	33.7	4.89	36.3	5.27	34.0	4.93
Diabase	30.5	4.42	32.3	4.69	35.3	5.12	33.0	4.78
Supplemental Cementitious Material Mixtures								
	7 Days		28 Days		90 Days		AASHTO	
	GPa	x 10⁶psi	GPa	x 10⁶psi	GPa	x 10⁶psi	GPa	x 10⁶psi
A4-D/FA	31.2	4.52	35.3	5.12	40.7	5.91	36.1	5.23
A4-D/MS	30.4	4.41	35.5	5.15	42.1	6.11	36.5	5.29
A4-D/S	33.3	4.83	37.0	5.37	42.3	6.14	38.0	5.51
A5-D/S	33.2	4.81	38.1	5.52	44.6	6.47	39.2	5.68

Unrestrained Shrinkage

Table 10 presents the average percent length change for unrestrained concrete specimens at 7, 28, 56, 90, 120, 150, and 180 days.

Table 10. Average Percentage Length Change

Mixture	7 Days	28 Days	56 Days	90 Days	120 Days	150 Days	180 Days
A3-Lstone	-0.0162	-0.0253	-0.0380	-0.0393	-0.0431	-0.0457	-0.0468
A3-Gravl.	-0.0186	-0.0280	-0.0367	-0.0370	-0.0432	-0.0459	-0.0462
A3-Diab.	-0.0183	-0.0286	-0.0392	-0.0458	-0.0490	-0.0507	-0.0541
Mixture	7 Days	28 Days	56 Days	90 Days	120 Days	150 Days	180 Days
A4-Lstone	-0.0139	-0.0217	-0.0342	-0.0378	-0.0401	-0.0415	-0.0442
A4-Gravl.	-0.0172	-0.0258	-0.0323	-0.0368	-0.0384	-0.0402	-0.0419
A4-Diab.	-0.0155	-0.0276	-0.0392	-0.0422	-0.0457	-0.0478	-0.0514
Mixture	7 Days	28 Days	56 Days	90 Days	120 Days	150 Days	180 Days
A5-Lstone	-0.0160	-0.0225	-0.0321	-0.0351	-0.0367	-0.0378	-0.0394
A5-Gravl.	-0.0153	-0.0266	-0.0328	-0.0366	-0.0380	-0.0396	-0.0415
A5-Diab.	-0.0180	-0.0256	-0.0364	-0.0427	-0.0453	-0.0465	-0.0494
Mixture	7 Days	28 Days	56 Days	90 Days	120 Days	150 Days	180 Days
A4-D/FA	-0.0197	-0.0396	-0.0487	-0.0522	-0.0537	-0.0547	-0.0561
A4-D/MS	-0.0187	-0.0367	-0.0433	-0.0447	-0.0473	-0.0490	-0.0510
A4-D/S	-0.0204	-0.0385	-0.0429	-0.0474	-0.0490	-0.0499	-0.0503
A5-D/S	-0.0198	-0.0354	-0.0425	-0.0457	-0.0478	-0.0491	-0.0500

Restrained Shrinkage

Table 11 presents the average microstrain ($\mu\epsilon$) values for the restrained concrete specimens at 7, 28, 56, 90, 120, 150, and 180 days. The average microstrain for the portland cement mixtures are the average of eight strain gages on two rings. The supplemental cementitious material microstrain is the average of 24 strain gages on six rings. The data and graphs for each of the individual mixtures are presented elsewhere (Mokarem, 2002).

Table 12 presents a summary of the restrained shrinkage specimens. It shows that those specimens that cracked within 180 days developed an estimated strain of greater than 200 microstrain, and those that did not developed a microstrain of 200 or less.

Table 11. Average Microstrain.

Mixture	7 Days	28 Days	56 Days	90 Days	120 Days	150 Days	180 Days
A3-Lstone	-63	-91	-164	-224	-234	-177	-179
A3-Gravl.	-71	-103	-127	-141	-123	-133	-139
A3-Diab.	-45	-57	-90	-106	-117	-125	-132
Mixture	7 Days	28 Days	56 Days	90 Days	120 Days	150 Days	180 Days
A4-Lstone	-54	-80	-127	-157	-162	-165	-168
A4-Gravl.	-56	-90	-142	-176	-183	-188	-194
A4-Diab.	-50	-110	-152	-179	-187	-193	-200
Mixture	7 Days	28 Days	56 Days	90 Days	120 Days	150 Days	180 Days
A5-Lstone	-59	-85	-118	-139	-142	-145	-148
A5-Gravl.	-61	-96	-132	-184	-194	-202	-149
A5-Diab.	-52	-83	-116	-164	-179	-201	-158
Mixture	7 Days	28 Days	56 Days	90 Days	120 Days	150 Days	180 Days
A4-D/FA	-60	-119	-136	-178	-184	-188	-193
A4-D/MS	-61	-93	-106	-141	-154	-163	-172
A4-D/S	-52	-83	-96	-122	-129	-136	-142
A5-D/S	-57	-103	-114	-125	-137	-148	-157

Table 12. Summary of Shrinkage (microstrain) and Age at Cracking

	Microstrain			Cracking	
	28 Days	90 Days	180 Days	Days	Est. $\mu\epsilon$
A3/PCC					
Limestone	-91	-224	---	125	-240
Gravel	-103	-141	---	117	-210
Diabase	-57	-106	-132	*	*
A4/PCC					
Limestone	-80	-157	-168	*	*
Gravel	-90	-176	-194	*	*
Diabase	-110	-179	-200	*	*
A5/PCC					
Limestone	-85	-139	-148	*	*
Gravel	-96	-184	---	172	-220
Diabase	-83	-164	---	165	-210
A4/SCM					
Fly Ash	-119	-178	-193	*	*
Microsilica	-93	-141	-172	*	*
Slag Cement	-53	-122	-142	*	*
A5/SCM					
Slag Cement	-103	-125	-157	*	*

* Specimens that have not cracked as of 180 days.

Prediction Models

The percent shrinkage was calculated for each of the five models at 7, 28, 56, 90, 120, 150, and 180 days after shrinkage had commenced. A residual value for each measured unrestrained shrinkage specimen was calculated as follows:

$$\text{Residual Value} = \text{Predicted Value} - \text{Measured (Experimental) Value} \quad (\text{Eq. 2})$$

Thus, if the residual value was positive, it indicated that the model overestimated the shrinkage. If the residual value was negative, it indicated that the model underestimated the shrinkage. The ACI 209 and Sakata models are applicable for only Type I general and Type III High early strength cements. Therefore, residuals were not calculated for the A4-diabase/fly ash, A4-diabase/slag cement, and A5-diabase/slag cement mixtures for the ACI 209 and Sakata models, because these cementing materials hydrate at a slower rate than a Type I or Type III cement. The residuals are an indication of the models' tendency to either overestimate or underestimate shrinkage. However, the residuals do not necessarily determine which model is the best predictor. A graphical representation of the residuals for each model can be found elsewhere (Mokarem, 2002). To determine which model is the best predictor, two analyses were performed: an error percentage analysis and a residual sum of squares. These analyses are discussed later in this report.

DISCUSSION AND ANALYSIS

This section presents a discussion of the test results including compressive strength, modulus of elasticity, and unrestrained and restrained shrinkage. An analysis of the five shrinkage prediction models is also presented.

Compressive Strength

One of the factors that contributes to the compressive strength of concrete is the water-to-cement (w/c) ratio of the mixture. In general, a mixture with a lower w/c ratio should produce a higher compressive strength.

The compressive strength results were in accord with the expected relationship of lower w/c ratios producing higher compressive strengths. For the A3 portland cement mixtures, the gravel mixtures had the lowest w/c ratios, and the highest compressive strengths. The gravel and diabase mixtures had similar w/c ratios and the corresponding compressive strengths were not significantly different. The limestone mixtures had the highest w/c ratio and lowest compressive strength and were significantly different from the gravel and diabase mixtures.

The A4 portland cement concrete mixture results were similar. The gravel mixtures had the lowest w/c ratio and the highest compressive strength. The gravel mixture compressive strengths were significantly greater than the diabase and limestone mixture compressive strengths.

The A5 portland cement concrete limestone, gravel, and diabase mixtures had w/c ratios of 0.33, 0.35, and 0.39, respectively. The limestone mixtures had the highest compressive strengths followed by the gravel mixtures and the diabase mixture's which had the lowest compressive strengths. The limestone, gravel, and diabase mixture compressive strengths were all significantly different from each other.

For the supplemental cementitious material mixtures, the A4 mixtures had a water-to-cementitious material (w/cm) ratio of 0.43 and the A5 mixture had a w/cm ratio of 0.39. The A5 mixture had the highest compressive strengths. For the A4 mixtures, the mixture with slag cement had a higher compressive strength than the mixtures with fly ash and microsilica.

The concrete mixture proportions for all of the study mixtures were VDOT-approved plant mixtures. The VDOT A3, A4, and A5 concrete compressive strength requirements are 20.7 MPa (3000 psi), 27.6 MPa (4000 psi), and 35.5 MPa (5000 psi) at 28 days. The mixture compressive strengths were significantly greater than the minimum specified strengths. For worst case conditions, the 28-day compressive strengths were 18 MPa (2680 psi), 8.6 MPa (1250 psi), and 12.9 MPa (1870 psi) greater than the minimum specified compressive strengths, respectively.

Modulus of Elasticity

Table 9 presented the average modulus of elasticity for the mixtures at 7, 28, and 90 days. The modulus of elasticity increases with increasing compressive strength. For the A3 and A4 portland cement mixtures, the modulus of elasticity for the limestone, gravel, and diabase mixtures were not significantly different.

For the A5 portland cement mixtures, the limestone mixtures had a significantly higher modulus of elasticity and corresponding compressive strength than the gravel and diabase mixtures. The supplemental cementitious material mixtures had significantly higher modulus of elasticity results than the portland cement concrete mixtures. This is the result of a denser bulk cement paste matrix and aggregate/cement paste transition zone than for the portland cement mixtures.

A comparison was also performed between the measured modulus of elasticity and the results of the equation used to determine modulus of elasticity by ACI 318 Building Code. The ACI equation is as follows:

$$E_c = 57,000\sqrt{f'_c} \quad (\text{Eq. 3})$$

where: E_c = modulus of elasticity ($\times 10^6$ psi)
 f'_c = average 28-day compressive strength (psi)

Figure 2 presents the comparison between the ACI 318 Building Code and the measured modulus of elasticity results.

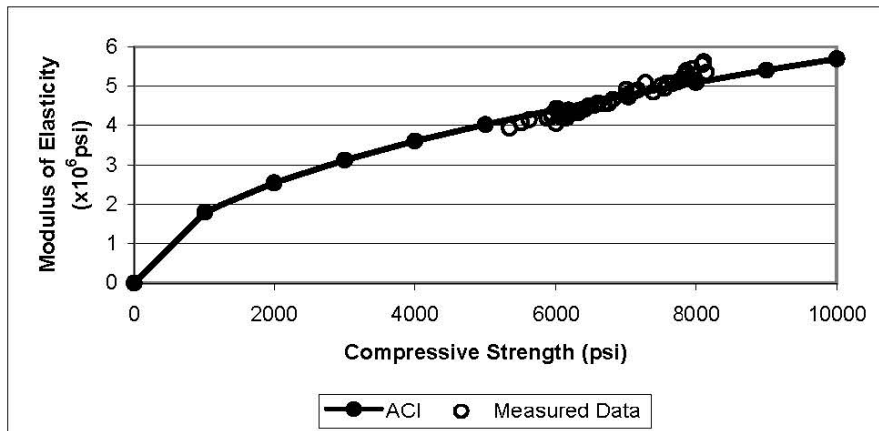


Figure 2. ACI 318 Building Code versus Measured Modulus of Elasticity

As shown in Figure 2, the measured modulus of elasticity results were within 10% of the ACI 318 Building Code values.

Unrestrained Shrinkage

Table 10 presented the average percent length change for unrestrained concrete specimens at 7, 28, 56, 90, 120, 150, and 180 days.

For the A3 portland cement concrete mixtures, the diabase specimens exhibited the highest percent length change. The limestone and gravel specimens had similar percent length changes, which were significantly less than the diabase values at later ages. For the first 56 days of drying, there was not a significant difference in the percent length change among the three mixtures. However, after 56 days of drying, the diabase specimens began to undergo greater percent length changes than the limestone and gravel specimens.

For the A4 portland cement concrete mixtures, the gravel mixtures exhibited the smallest percent length change. Again, the diabase mixture exhibited the highest percentage length change. The gravel mixtures had a w/c ratio of 0.42, and the limestone and diabase mixtures had w/c ratios of 0.45 and 0.43, respectively. The gravel and limestone mixtures were in accord with the general relationship that a lower w/c ratio produces lower shrinkage; however, the diabase mixture had a lower w/c ratio than the limestone and exhibited higher shrinkage. There was not a significant difference between the percent length change values for the limestone and gravel mixtures. However, both the limestone and gravel percent length changes were significantly less than those of the diabase mixtures.

The A5 portland cement concrete mixtures had a greater range of w/c ratios than the A3 and A4 mixtures. The w/c ratios were 0.33, 0.35, and 0.39 for the limestone, gravel, and diabase mixtures, respectively. The limestone mixtures, which had the lowest w/c ratio, exhibited the lowest shrinkage, and the diabase mixtures, with the highest w/c ratio, exhibited the highest amount of shrinkage. The limestone and gravel percent length change values were not significantly different, but they were both significantly lower than for the diabase mixtures.

Overall, for the portland cement concrete mixtures, the diabase mixtures consistently exhibited higher shrinkage than the limestone and gravel mixtures. It appears that the aggregate type has an effect on the drying shrinkage. One of the factors that may influence shrinkage is the absorption of the aggregate. The fine aggregate used with the diabase aggregate had an absorption value of 1.04%, whereas the absorption values of the limestone and gravel fine aggregate were 0.48% and 0.75%, respectively. A higher absorption value indicates that a higher percent of aggregate voids are filled with water, which may lead to an increase in drying shrinkage. Another factor that may influence shrinkage is the modulus of elasticity of the aggregate. A lower aggregate modulus of elasticity would result in a lower restraining effect on the cement paste during drying shrinkage.

For the supplemental cementitious material mixtures, the mixture containing the fly ash exhibited the greatest amount of shrinkage. The mixtures containing microsilica and slag cement were not significantly different. The A4 mixtures containing supplemental cementitious materials had the same w/c ratio and aggregate type: diabase.

The w/c ratios for the A4 and A5 slag cement mixtures were 0.43 and 0.39, respectively. For the slag cement mixtures, the w/c ratio did not have a significant effect on shrinkage.

The supplemental cementitious material mixtures exhibited greater drying shrinkage than the associated portland cement concrete mixtures. This could be due to the denser matrix produced by the fly ash, microsilica, and slag cement. This denser matrix would create smaller capillary voids, and the bulk of drying shrinkage in concrete occurs from the loss of water from the smaller capillary voids.

Restrained Shrinkage

Table 11 presented the average microstrain ($\mu\epsilon$) values for the restrained concrete specimens at 7, 28, 56, 90, 120, 150, and 180 days.

For the A3 portland cement concrete mixtures, the limestone mixture exhibited the greatest microstrain followed by the gravel and diabase mixtures. Concrete rings from the limestone and gravel mixtures experienced cracking, whereas rings from the diabase mixture did not crack. One of the concrete rings from the limestone mixture cracked after 125 days. The measured average microstrain value for that ring was -234 microstrain at 120 days. Thus, the ring cracked after an average microstrain of slightly greater than -234 . One of the rings from the gravel mixture also cracked, the ring cracked; after 117 days. The average microstrain for this ring was -141 after 90 days. The estimated microstrain was -210 at cracking. The diabase mixture rings did not crack during the test period of 180 days. The average microstrain for these rings was -132 at 180 days. This was significantly less strain than was experienced by the limestone and gravel rings. The modulus of elasticity for the limestone and gravel mixtures was higher than for the diabase mixture. This may have been a factor in the cracking of the limestone and gravel rings. With a higher modulus, the concrete is stiffer and it may be able to resist shrinkage in an unrestrained condition. However, in a restrained condition, the stiffer concrete may create higher strains on the ring.

For the A4 portland cement concrete mixtures, none of the rings experienced cracking. The diabase rings experienced the greatest amount of strain, and the limestone rings experienced the least. The average microstrain results at 180 days were -168 , -194 , and -200 for the limestone, gravel, and diabase, respectively. The modulus of elasticity for the gravel and diabase mixtures was higher than for the limestone mixtures, which may account for the higher restrained shrinkage strains.

For the A5 portland cement concrete mixtures, the gravel and diabase mixtures experienced cracking. One of the diabase rings cracked after 165 days; the most recent average microstrain reading for that ring was -201 at 150 days. The estimated microstrain at cracking was -210 . The same was true for the gravel mixture. One of the rings cracked after 172 days with the most recent average microstrain reading being -202 at 150 days. The estimated microstrain cracking was -210 . One of the factors that may have influenced the cracking tendency of the A5 portland cement concrete mixtures was the w/c ratio of the mixtures. The w/c ratios were 0.33, 0.35, and 0.39 for the limestone, gravel, and diabase, respectively. The lower w/c ratio should produce less shrinkage, which in turn may produce less strain. Throughout the testing of the A5 mixtures, the limestone mixture, which had the lowest w/c ratio, exhibited significantly less strain.

None of the supplemental cementitious material rings experienced cracking. The average microstrain values ranged from -142 to -193 , with the fly ash mixtures experiencing the highest strain and the A4 slag cement mixture experiencing the least strain. The A4 and A5 slag cement mixtures had less strain than the microsilica and fly ash mixtures. It should be noted that the fly ash mixtures experienced higher shrinkage for both the unrestrained and restrained conditions. Thus, it appears that an average microstrain in excess of -200 will result in the cracking of the restrained drying shrinkage rings.

Relationship Between Percentage Length Change and Microstrain

A total of 42 ring specimens were fabricated for this study, and only 4 of the rings experienced cracking. However, all of the rings that cracked had average microstrain values in excess of $-200 \mu\epsilon$. Therefore, it appears that if the strain produced in a restrained situation is greater than $200 \mu\epsilon$, there is an increased probability of cracking. The percentage length change was plotted versus the microstrain for each mixture to determine if there was a correlation. The values were from measurements taken at 7, 28, 56, 90, 120, 150, and 180 days. Figure 3 presents the percent length change versus microstrain for the A3 portland cement concrete mixtures.

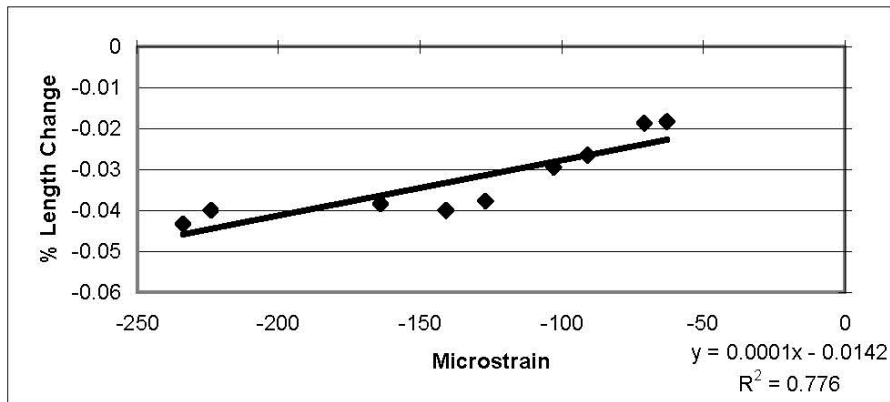


Figure 3. Percentage Length Change vs. Microstrain for A3 Portland Cement Concrete Mixtures

For the A3 portland cement concrete mixtures, there is a fairly strong correlation between the percentage length change and microstrain. If the value of $-200 \mu\epsilon$ is used in the linear equation from Figure 3, a value of -0.0342 would be obtained for the percentage length change. Since there is a higher probability for cracking when the strain value is greater than $200 \mu\epsilon$, the probability for cracking is increased if the percent length change is greater than 0.0342 .

Figure 4 presents the percent length change versus microstrain for the A4 portland cement concrete mixtures.

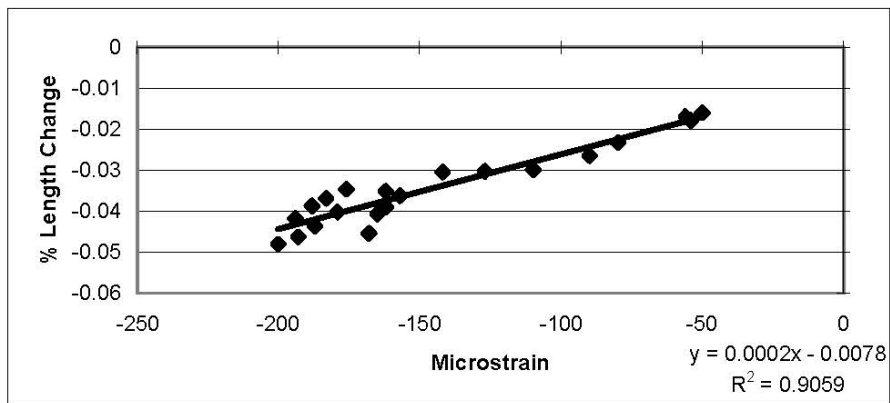


Figure 4. Percentage Length Change vs. Microstrain for A4 Portland Cement Concrete Mixtures

There is a stronger correlation between percentage length change and microstrain for the A4 portland cement concrete mixtures. Using a value of $-200 \mu\epsilon$ in the linear equation from Figure 4, gives a value of -0.0478 for the percentage length change. This would mean that if the percent length change is greater than 0.0478 , there is an increased probability of cracking.

Figure 5 presents the percentage length change versus microstrain for the A5 portland cement concrete mixtures.

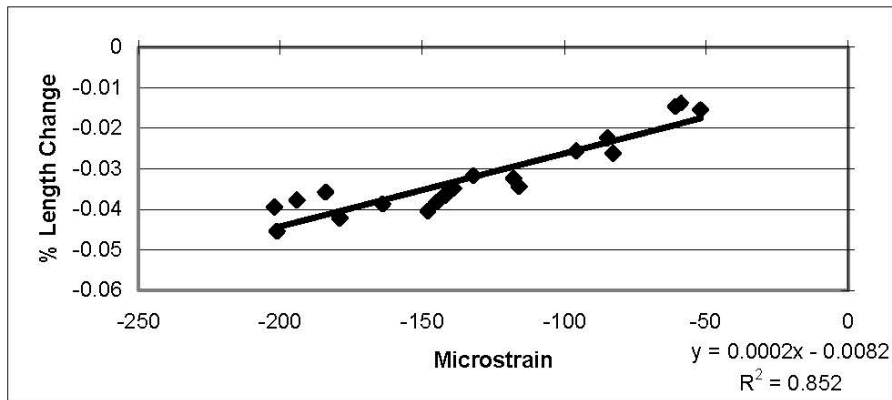


Figure 5. Percentage Length Change vs. Microstrain for A5 Portland Cement Concrete Mixtures

For the A5 portland cement concrete mixtures, there is a strong correlation between the percentage length change and microstrain. Using a value of $-200 \mu\epsilon$ in the linear equation from Figure 5 gives a value of -0.0482 for the percentage length change. Thus, if the percent length change is greater than 0.0482 , there is an increased probability of cracking.

Figure 6 presents the percentage length change versus microstrain for the supplemental cementitious material mixtures. Note that these mixtures used the same aggregate type, diabase, and the associated fine aggregate. Also the water to cement plus pozzolan ratios were the same, 0.43 .

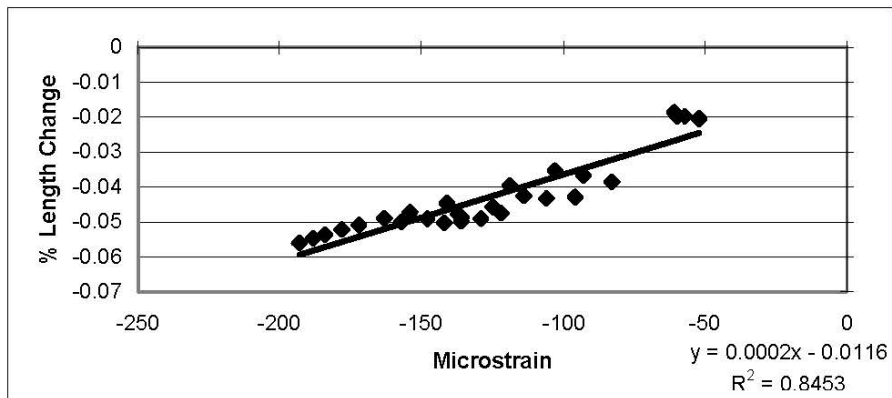


Figure 6. Percentage Length Change vs. Microstrain for Supplemental Cementitious Material Mixtures

For the supplemental cementitious material concrete mixtures there is a strong correlation between the percentage length change and microstrain. Using a value of $-200 \mu\epsilon$ in the linear equation from Figure 6, you would obtain a value of -0.0516 for the percentage length change. Thus, if the percentage length change is greater than 0.0516 , there is an increased probability of cracking for these mixtures.

Based on the results obtained from the correlation between percentage length change and microstrain, a performance specification can be developed. It has been shown that if the microstrain in the restrained shrinkage specimens is greater than $200\mu\epsilon$, there is an increased

probability of cracking. The associated percentage length change was calculated from linear equations for each mixture group. It appears that the percent length change for the portland cement concrete mixtures is between 0.0342 and 0.0485 for a restrained shrinkage of 200µε. Therefore, if the percent length change for the portland cement concrete mixtures is limited to 0.0300 at 28 days and 0.0400 at 90 days, there is a reduced probability of cracking due to drying shrinkage. For the supplemental cementitious material mixtures, at restrained shrinkage of 200µε, the associated percent length change is 0.0516. Therefore, if the percentage length change is limited to 0.0400 at 28 days and 0.500 at 90 days for these mixtures, there is a reduced probability of cracking due to drying shrinkage.

Table 13 presents a comparison of the proposed performance specification and other proposed performance specifications. The other performance specifications were proposed for the Fairfax County Water Authority, the Port Authority of New York and New Jersey (2000).

Table 13. Comparison of Performance Specifications

Source	Percentage Length Change Limits		
	At 21 Days	At 28 Days	At 90 Days
Fairfax County Water Authority (Laboratory)	0.0360-0.0480	---	---
Fairfax County Water Authority (Field)	0.0480-0.0640	---	---
Port Authority of New York and New Jersey	---	0.0400	---
Current Study (VDOT) PCC	---	0.0300	0.0400
Current Study (VDOT) SCM	---	0.0400	0.0500

As shown, the majority of the performance specifications limits the percentage length change to 0.0400 at 28 days. The Fairfax County Water Authority has limits at 21 days. The limits are for both lab and field mixtures. For the lab mixtures, the percentage length change limit is 0.0360 for concrete to be used in liquid-containing structures and 0.0480 for concrete to be used in other structures. For the field mixtures, the percentage length change limits are 0.0480 and 0.0640 for liquid-containing and other concrete structures, respectively. All of the shrinkage tests were performed in accordance with ASTM C157.

Prediction Model Analysis

Five shrinkage prediction models were analyzed in this study:

1. ACI – 209 Code Model (ACI 209)
2. Bazant Model B3 (Bazant)
3. Comite Euro-International Du Beton Model Code 1990 (CEB90)
4. Gardner – Lockman Model (Gardner/Lockman)
5. Sakata Model (Sakata)

The residuals were calculated for each individual model for each mixture. These residual values are an indication of the models ability to either overestimate or underestimate shrinkage. However, the residuals do not necessarily determine which model is the best predictor. To determine which model is the best predictor, two analyses were performed: an error percentage analysis and a summation of the residuals squared. The error percentage was calculated as follows for the residual values at 7, 28, 56, 90, 120, 150, and 180 days:

$$\text{Error Percentage} = \frac{\text{Residual} * 100}{\text{Experimental Value}} \text{ (Eq. 4)}$$

The error percentage values as a function of time are presented elsewhere (Mokarem, 2002). An average error percentage for the seven time periods was calculated; a smaller error percentage over the 180-day time period indicates a better fit model.

For the summation of the residuals, squared the model with the smallest value indicates the best predictor.

Error Percentage Analysis

Portland Cement Concrete Mixtures

Table 14 presents the rank order of the average error percentage for each model for the limestone, gravel, and diabase portland cement concrete mixtures.

Table 14. Average Error Percentage for Limestone, Gravel, and Diabase Mixtures

Prediction Model	Limestone	Gravel	Diabase
CEB 90	22	17	10
Bazant	25	17	11
Gardner/Lockman	26	19	12
ACI 209	42	40	25
Sakata	80	72	57

As shown, the rank order was the same for the three aggregate types with little difference among the CEB 90, Bazant, and Gardner/Lockman models. The average error percentage results indicated that the ACI 209 and Sakata models were not as accurate.

The rank order from best to worst fit among aggregate types was diabase, gravel, and limestone. However, all of the models overestimated the shrinkage during the 180-day test period. Note that the diabase mixtures, which had displayed the greatest amount of shrinkage, had the lowest error percentage for the CEB 90, Bazant, and Gardner/Lockman models: 10, 11, and 12 percent, respectively.

Supplemental Cementitious Material Mixtures

Table 15 presents the models' average error percentages for the supplemental cementitious material mixtures.

Table 15. Average Error Percentage for Supplemental Cementitious Material Mixtures

Prediction Model	A4-D/FA	A4-D/MS	A4-D/S	A5-D/S
Gardner/Lockman	20	14	13	67
CEB 90	30	25	24	78
Bazant	30	24	22	78
ACI 209	---	---	---	110
Sakata	---	---	---	145

For the fly ash and slag cement mixtures, the Bazant, CEB 90, and Gardner/Lockman models were used in the shrinkage prediction analyses because these cementing materials are closer in hydration characteristics to a Type II cement rather than a Type I.

The Bazant, CEB 90, and Gardner/Lockman models include an adjustment factor for cement types, whereas the ACI 209 and Sakata models do not consider the influence of various cementing materials.

As shown in Table 15, the rank order of the best to worst prediction model for the A4 fly ash and the A4 and A5 slag cement mixtures was the Gardner/Lockman model, with the CEB 90 and Bazant models being equivalents. The ACI 209 and Sakata models were not as accurate for the A4 microsilica mixture.

Overall, for the error percentage analysis of the data, the models tended to overestimate the shrinkage of the portland cement concrete mixtures and underestimate the shrinkage of the supplemental cementitious material mixtures. One likely reason, which will be discussed further in the sensitivity analysis of these models at the end of this section, is that these models predict shrinkage largely based on the average 28-day compressive strength of the mixture. This parameter does not directly account for the pore volume and pore size distribution of the mixture, which greatly affects drying shrinkage. For the portland cement concrete mixtures, the CEB 90 model was the best predictor followed closely by the Bazant and Gardner/Lockman models. The Sakata model was the worst predictor for these mixtures. For the supplemental cementitious material mixtures, the Gardner/Lockman model was the best predictor. It was consistently better than the Bazant and CEB 90 models for the mixtures that were considered to be type II cement.

Residual Sum of Squares Analysis

Portland Cement Concrete Mixtures

Figure 7 presents the residual sum of squares analysis for the limestone, gravel, and diabase portland cement concrete mixtures. A lower total summation indicates that the model is a better predictor.

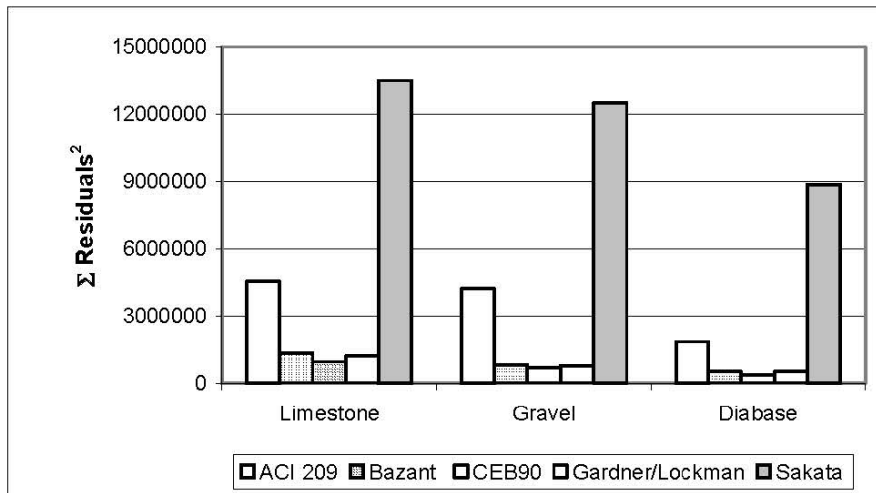


Figure 7. Residual Sum of Squares for Limestone, Gravel, and Diabase Mixtures

For the limestone portland cement concrete mixtures, the values demonstrated that the CEB 90 model was the best predictor of shrinkage. It was followed closely by the Gardner/Lockman and Bazant models.

For the gravel portland cement concrete mixtures, the CEB 90 model was the again the best predictor based on the residual sum of squares values. The Gardner/Lockman and Bazant models followed closely. The ACI 209 and Sakata models performed significantly worse for these mixtures.

For the diabase portland cement concrete mixtures, the values demonstrated that the CEB 90 model was the best predictor of shrinkage. The Gardner/Lockman and Bazant models were similar in predicting shrinkage and closely resembled the CEB 90 model.

Supplemental Cementitious Material Mixtures

Figures 8 and 9 present the residual sum of squares values for the supplemental cementitious material mixtures. Figure 8 presents the values for the fly ash and slag cement mixtures. Figure 9 presents the values for the microsilica mixture.

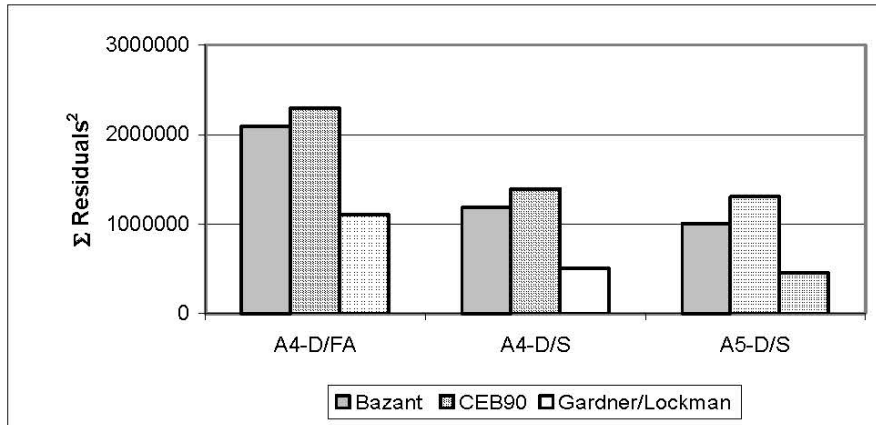


Figure 8. Residual Sum of Squares for Fly Ash and Slag Cement Mixtures

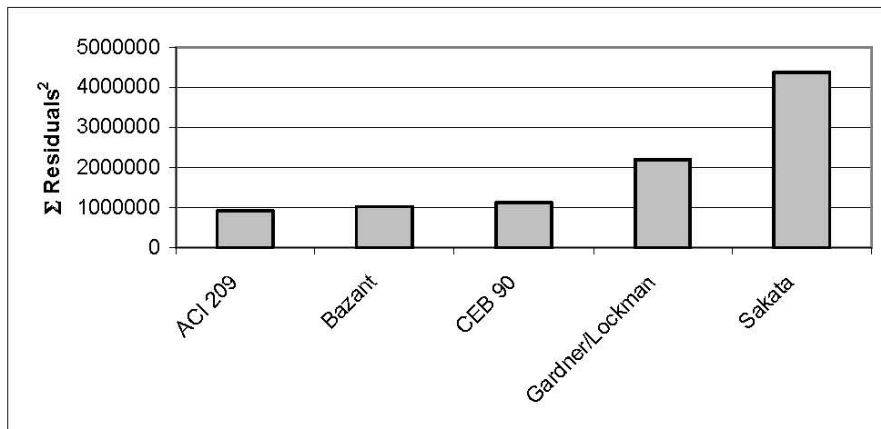


Figure 9. Residual Sum of Squares for Microsilica Mixture

For the fly ash and slag cement mixtures, only the Bazant, CEB 90, and Gardner/Lockman models were analyzed because of limitations on cement type for the ACI 209 and Sakata models.

For the fly ash mixtures, the Gardner/Lockman model was the best predictor followed by the Bazant and CEB 90 models. The values for the A4 slag cement mixture demonstrated that the Gardner/Lockman model was the best predictor, followed by the Bazant and CEB90 models. The same was true for the A5 slag cement mixtures.

For the microsilica mixture, the values demonstrated that the ACI 209 model was the best predictor. The Bazant and CEB 90 models followed closely. The Gardner/Lockman model was the fourth best predictor. These mixtures were considered to be Type I cement mixtures. The ACI 209 and Sakata models overestimated the shrinkage, and the Bazant, CEB 90, and Gardner/Lockman models underestimated the shrinkage. The same analysis was performed assuming that the mixtures were a Type II cement. In this case, the Gardner/Lockman model was the best predictor. The reason for the skewed results using a Type I cement analysis is that the actual measured shrinkage values were high and the models are strongly based on

compressive strength. The models assume that a higher 28-day compressive strength will be associated with less shrinkage; however, that may not be true.

Summary of Error Percentage and Summation of the Residuals Squared Analysis

The error percentage and summation of the residuals squared analyses demonstrated the same results in terms of the model performance from best to worst. For the portland cement concrete mixtures, the models overestimated shrinkage, whereas supplemental cementitious material mixtures, the models underestimated shrinkage. The CEB 90 model was the best predictor for the portland cement concrete mixtures, and the Gardner/Lockman model was the best predictor for the supplemental cementitious material mixtures. It should be noted that the portland cement concrete mixtures were analyzed using a Type I cement and the supplemental cementitious material mixtures were analyzed using a Type II cement. The Bazant, CEB 90, and Gardner/Lockman models were used for the Type II cement analysis, with each having a correction factor for Type II cement. These correction factors varied among the models.

As mentioned previously, the models predict shrinkage largely based on the 28-day compressive strength of a mixture. A lower compressive strength results in a higher predicted shrinkage for these models. The compressive strength parameter is used in an effort to account for the effects of water and cement; a lower w/c ratio should indicate a lower water content, thus less shrinkage. Although compressive strength influences the amount of shrinkage, there are other factors that need to be considered. These factors include the pore volume and pore size distribution. The majority of drying shrinkage is associated with the loss of water from the smaller capillary voids in the concrete. A concrete mixture using supplemental cementitious materials such as fly ash, microsilica, and slag cement has a more refined pore structure than ordinary portland cement concrete mixtures. There are more smaller capillary voids in these mixtures, and the removal of water from these voids may result in more shrinkage.

From the results obtained in this study, it appears that the type of aggregate may also influence shrinkage. In this study, the mixtures using diabase as the aggregate consistently had more shrinkage than mixtures using limestone or gravel as the aggregate. The fine aggregate used with the diabase aggregate had higher absorption values than those used with the limestone and gravel aggregate. The absorption values for the fine aggregate were 0.48, 0.75, and 1.04 for the limestone, gravel, and diabase, respectively. This may have contributed to the higher shrinkage values in the sense that the fine aggregate used with the diabase aggregate, which absorbs more water than the the fine aggregate used with the limestone and gravel aggregate, would shrink more during drying.

Prediction Model Sensitivity Analysis

Based on the results of this study, a sensitivity analysis was performed on the three best predictors: the Bazant, CEB 90, and Gardner/Lockman models. This analysis took into consideration the parameters for each of these models and how the predicted values would change over time based on changing one factor while leaving the other factors constant. The predicted shrinkage was calculated at 28, 56, 90, and 180 days for each model. The factors that

were common to all three models were 28-day compressive strength and relative humidity. The Bazant model includes a water content parameter.

Bazant B3 Model Sensitivity Analysis

The three factors that were analyzed for the Bazant model were 28-day compressive strength, water content, and relative humidity. Figure 10 presents the sensitivity of the predicted shrinkage as a function of compressive strength, keeping the water content (10 pcf) and relative humidity (50%) constant.

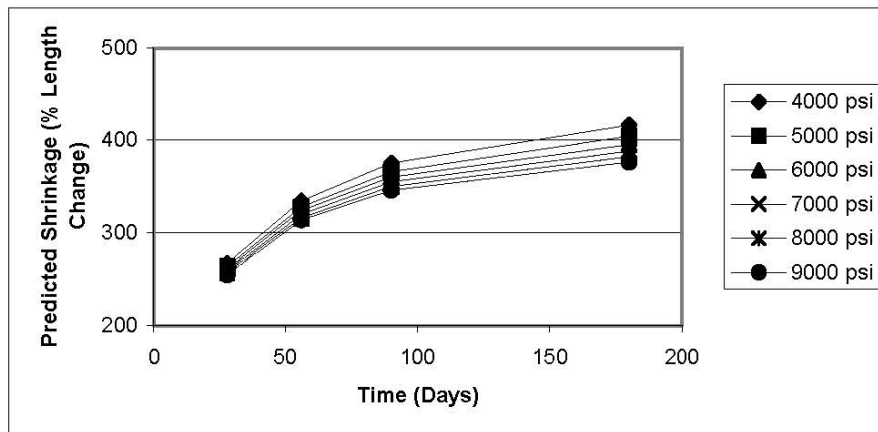


Figure 10. Bazant Sensitivity as a Function of Compressive Strength (Water Content, Relative Humidity Constant)

Figure 10 shows that the 28-day compressive strength has an increasing effect on predicted shrinkage with increasing time. However, the predicted shrinkage values do not appear to be significantly different, even at 180 days. Therefore, it does not appear that 28-day compressive strength has a significant effect on the predicted shrinkage values.

Figure 11 presents the sensitivity of the predicted shrinkage as a function of water content while keeping the compressive strength constant at 5000 psi and the relative humidity at 50%.

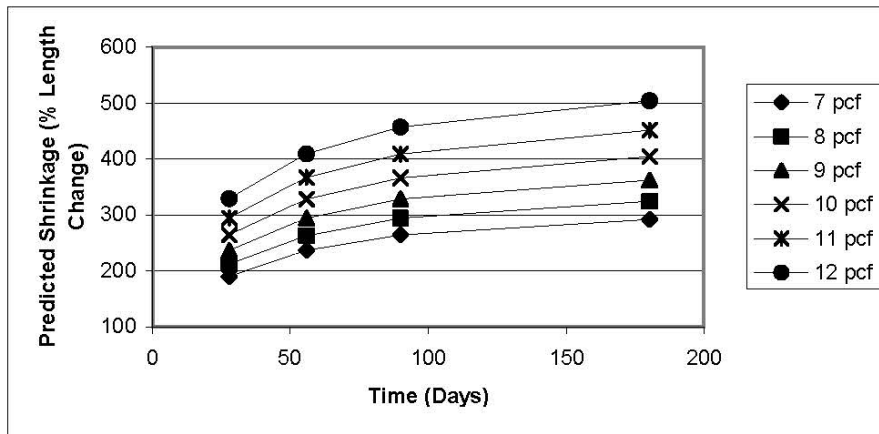


Figure 11. Bazant Sensitivity as a Function of Water Content (Compressive Strength=5000 psi, Relative Humidity=50%)

Figure 11 shows that changing water content has a greater effect on the predicted shrinkage than changing the 28-day compressive strength presented in Figure 10. This further reinforces the fact that the 28-day compressive strength has little effect on the predicted shrinkage value. Figure 11 also shows that changing the water content has an increasing effect on the predicted shrinkage value as time increases.

Figure 12 presents the sensitivity of the predicted shrinkage as a function of relative humidity while keeping the compressive strength constant at 5000 psi and the water content at 10 pcf.

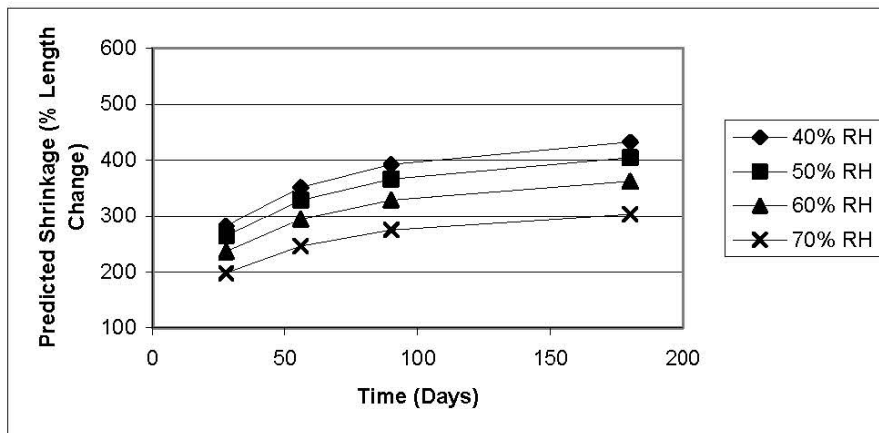


Figure 12. Bazant Sensitivity as a Function of Relative Humidity (Compressive Strength=5000 psi, Water Content=10 pcf)

Figure 12 shows that changing relative humidity also has a greater effect on the predicted shrinkage than changing the 28-day compressive strength presented in Figure 10. Figure 12 also shows that changing the relative humidity has an increasing effect on the predicted shrinkage value as time increases. It should also be noted that the difference in changing the relative

humidity is less as the relative humidity decreases. The reason for this is that below 50% relative humidity, there is less moisture in the system that can be removed by drying.

Of the three factors that were analyzed for sensitivity for the Bazant model, changing water content had the greatest effect on predicted shrinkage values. The changing of the relative humidity also had an effect on the predicted shrinkage values; however, it was not as significant as changing the water content. Changing the 28-day compressive strength had virtually no effect on the predicted shrinkage values.

CEB90 Model Sensitivity Analysis

Two factors were analyzed for sensitivity analysis of the CEB 90 model parameters: the 28-day compressive strength and relative humidity. Figure 13 presents the sensitivity of the predicted shrinkage as a function of compressive strength, keeping the relative humidity constant at 50%.

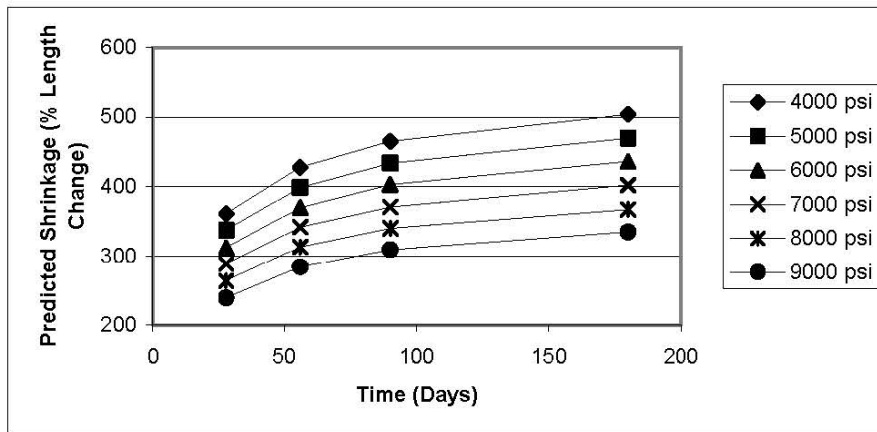


Figure 13. CEB90 Sensitivity as a Function of Compressive Strength (Relative Humidity Constant at 50%)

Figure 13 shows that changing the 28-day compressive strength has an effect on the predicted shrinkage values for the CEB 90 model. The change appears to be the same for each increment of 1000 psi increase in compressive strength.

Figure 14 presents the sensitivity of the predicted shrinkage values for the CEB 90 model when changing the relative humidity while keeping the 28-day compressive strength constant at 5000 psi.

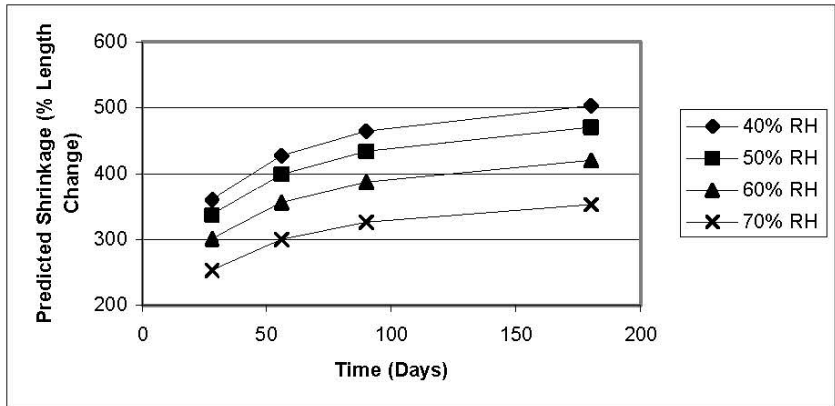


Figure 14. CEB 90 Sensitivity as a Function of Relative Humidity (Compressive Strength Constant at 5000 psi)

Figure 14 shows that changing the relative humidity for the CEB 90 model does have an effect on the predicted shrinkage value over time. Again, it is shown that as the relative humidity decreases, the effect on the predicted shrinkage value is less.

Gardner/Lockman Model Sensitivity Analysis

The two factors analyzed for sensitivity analysis of the Gardner/Lockman model were the 28-day compressive strength and relative humidity. Figure 15 presents the sensitivity of the predicted shrinkage as a function of compressive strength, keeping the relative humidity constant at 50%.

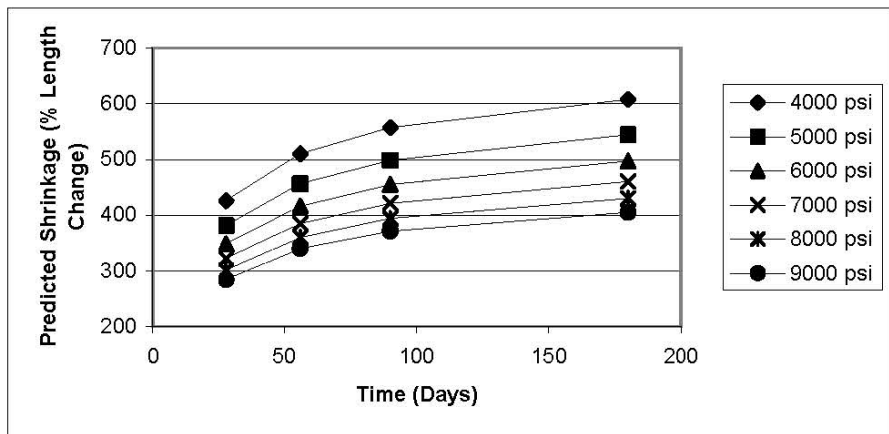


Figure 15. Gardner/Lockman Sensitivity as a Function of Compressive Strength (Relative Humidity Constant at 50%)

Figure 15 shows that changing the 28-compressive strength for the Gardner/Lockman model does have an effect on the predicted shrinkage values. The model is more sensitive at lower compressive strengths; there is a greater change between 4000 psi and 5000 psi than there is between 8000 psi and 9000 psi. The model is also more sensitive at later ages.

Figure 16 presents the sensitivity of the predicted shrinkage values of the Gardner/Lockman model when changing the relative humidity while keeping the 28-day compressive strength constant at 5000 psi.

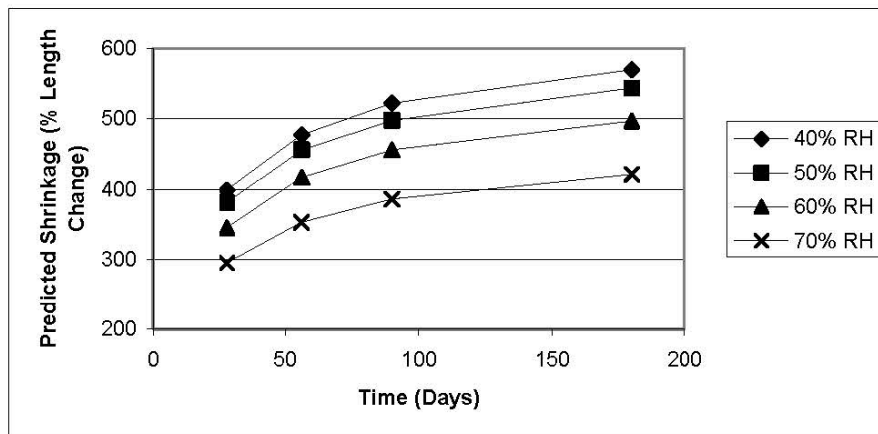


Figure 16. Gardner/Lockman Sensitivity as a Function of Relative Humidity (Compressive Strength Constant at 5000 psi)

Figure 16 shows that the predicted shrinkage values for the Gardner/Lockman model are sensitive to changes in humidity over time. The changes are more sensitive at higher relative humidities and lower compressive strengths. As with the CEB 90 model, the Gardner/Lockman model is more sensitive when changing the relative humidity is coupled with lower compressive strengths.

Summary of Prediction Model Sensitivity Analysis

The model sensitivity analyses demonstrate which parameters have the greatest effect on the predicted shrinkage values. The Bazant model was most sensitive to changes in the water content. This is in agreement with the concept of higher water losses from the smaller pores producing a greater amount of shrinkage. However, Bazant uses the 28-day compressive strength as a parameter, yet this parameter has little or no effect on the predicted shrinkage value. For concrete mixtures, there is a real question on the independence of water content and w/c ratio. Prediction improvement may be accomplished by dropping the strength parameter and incorporating a more sensitive pore characteristic parameter for various groups of cementing materials.

The CEB 90 and Gardner/Lockman models are sensitive to changes in compressive strength. From these models, a lower compressive strength will produce a greater amount of shrinkage. Lower compressive strength is an indication of a higher w/c ratio, which means that the mixture has a large water content. Here again, the models may be improved by replacing compressive strength with a parameter that better reflects the influence of pore characteristics (volume and size distribution). A possible parameter would be a permeability-age function. Although the loss of water from the concrete pore system is a diffusion process, diffusion and permeability are related for saturated systems.

From the data obtained in this study, the compressive strength and water content do influence the amount of shrinkage; however, there seems to be other factors that have an influence on the shrinkage. The supplemental cementitious material mixtures had higher compressive strengths than the portland cement concrete mixtures. They also had a greater amount of shrinkage. According to the prediction models, they should have less shrinkage. One of the reasons for the greater shrinkage in these mixtures is probably the denser matrix of the system. As mentioned previously, the supplemental cementitious material mixtures have more small capillary voids than do the ordinary portland cement concrete mixtures. The removal of water from these smaller capillary voids contributes more to the amount of shrinkage in the system than the removal of water from the larger voids.

Another factor that appears to influence shrinkage in this study is the type of aggregate used in the mixture. The diabase aggregate, with higher absorption values, consistently showed a greater amount of shrinkage than the mixtures using limestone and gravel aggregate. This could be due to the diabase aggregate contributing more to the water loss from the system than do the limestone and gravel aggregate.

It appears that the models try to take into account the void structure through the use of compressive strength and water content. However, the amount of shrinkage is influenced the most by the removal of water from the smaller capillary voids, and compressive strength is more an indication of the volume of the voids and not the pore size distribution. As for the influence of the aggregate on shrinkage, the models do not address the physical properties of the aggregate, such as absorption, that may have an influence on the amount of shrinkage.

CONCLUSIONS

1. The portland cement concrete mixtures containing diabase as the aggregate consistently exhibited greater drying shrinkage than the mixtures containing limestone and gravel as the aggregate.
2. The type of aggregate used in a mixture had an influence on the drying shrinkage of the mixture.
3. The mixtures containing fly ash exhibited greater drying shrinkage than those containing microsilica and slag cement.
4. There is a correlation between the percentage length change for unrestrained shrinkage specimens and microstrain for restrained shrinkage specimens. Thus, the unrestrained shrinkage test may be used as a performance-based specification for restrained concrete systems.
5. Based on the results of this study, the percentage length change for the portland cement concrete specimens should be limited to 0.0300 at 28 days and 0.0400 at 90 days to reduce the probability of cracking due to drying shrinkage.

6. Based on the results of this study, the percentage length change for the supplemental cementitious material mixtures should be limited to 0.0400 at 28 days and 0.0500 at 90 days to reduce the probability of cracking due to drying shrinkage.
7. The CEB 90 model is the best predictor of drying shrinkage for the portland cement concrete mixtures followed, closely by the Bazant, Gardner/Lockman, and then the ACI 209 and Sakata models.
8. The Gardner/Lockman model is the best predictor of drying shrinkage for the fly ash and slag cement mixtures followed by the Bazant, and CEB 90 models.

RECOMMENDATIONS

1. The unrestrained shrinkage test method, ASTM C 157, may be used as a performance-based specification for restrained concrete systems for concrete mixtures purchased by the Virginia Department of Transportation.
2. The percentage length change should be limited to 0.0300 at 28 days and 0.0400 at 90 days for portland cement concrete mixtures and 0.0400 at 28 days and 0.0500 at 90 days for supplemental cementitious material mixtures purchased by the Virginia Department of Transportation. This will aid in reducing the probability of cracking due to drying shrinkage.
3. Measurements should be continued on the existing unrestrained shrinkage specimens fabricated in this study to obtain percentage length changes at later ages.
4. Further research is needed in the area of aggregate influence on drying shrinkage.
5. Further research is needed on the influence of the pore size distribution of the cement paste on drying shrinkage.
6. There is a need to develop a prediction model that takes into account the aggregate influence and cement paste pore size distribution on drying shrinkage.

REFERENCES

- American Association of State Highway Transportation Officials, Standard Specification, 1996.
- Babaei, K. and Purvis, R.L., Minimizing Premature Cracking in Concrete Bridge Decks, Wilbur Smith Associates, Falls Church, Virginia, IBC-96-72, pp. 411-420, 1996.
- Bazant, Z.P., Creep and Shrinkage Prediction Model for Analysis and Design of Concrete Structures – Model B3, Materials and Structures, Vol. 28, 1995.

- Bhal, N.S., and Jain, J.P., Effect of Age at the Time of Loading on Creep of Concrete, Indian Concrete Journal, January 1996.
- Bhal, N.S., and Mital, M.K., Effect of Relative Humidity on Creep and Shrinkage of Concrete, Journal of the American Ceramic Society, Vol. 70, 1987, pp. 329-332.
- Brown, M.C., Corrosion Protection Service Life of Epoxy Coated Reinforcing Steel in Virginia Bridge Decks, Dissertation, Virginia Tech, Blacksburg, May 2002.
- Carlton, D., and Mistry, N., Thermo-Elastic-Creep Analysis of Maturing Concrete, Computers and Structures, Vol. 40, No. 2, 1991, pp. 293-302.
- DeLarrard, F., Acker, P., and Leroy, R., Shrinkage and Thermal Properties, 1994.
- Dilger, W.H., and Wang, C., Shrinkage and Creep of High Performance Concrete (HPC) – A Critical Review, 1998.
- Fairfax County Water Authority, Project 01800-6, CAST-IN-PLACE CONCRETE, Fairfax, 1997.
- Gardner, N.J., and Lockman, M.J., Design Provisions for Drying Shrinkage and Creep of Normal-Strength Concrete, ACI Materials Journal, Vol. 98, March-April 2001, pp. 159-167.
- Hansen, W., Constitutive Model for Predicting Ultimate Drying Shrinkage of Concrete, Journal of the American Ceramics Society, Vol. 70, pp. 329-332, 1987a.
- Hansen, W., Drying Shrinkage Mechanisms in Portland Cement Paste, Journal of the American Ceramics Society, Vol. 70, pp. 323-328, 1987b.
- Hau, C., Acker, P., and Ehlacher, A., Analysis and Models of the Autogenous Shrinkage of Hardened Cement Paste, Cement and Concrete Research, Vol. 25, No. 7, 1995.
- Holt, E., and Janssen, D., Influence of Early Age Volume Changes on Long Term Concrete Shrinkage, Transportation Research Board, Washington, D.C., 1998.
- McDonald, J.E., Vaysburd, A.M., Emmons, P.H., Poston, R.W., and Kesner, K.E., Selecting Durable Repair Materials: Performance Criteria-Summary, Concrete International, Vol. 24, No. 1, pp. 37-44, January 2000.
- Mehta, P.K., and Monteiro, P.J.M., Concrete Structure, Properties, and Materials, First Edition, Prentice Hall, Englewood Cliffs, New Jersey, 1986.
- Mehta, P.K., and Monteiro, P.J.M., Concrete Structures, Properties and Materials, Second Edition, Prentice Hall, Englewood Cliffs, New Jersey, 1993.

- Mindness, S., and Young, F., Concrete, Prentice Hall, Englewood Cliffs, New Jersey, 1981.
- Mokarem, D.W., Development of Concrete Shrinkage Performance Specifications, Dissertation in Civil and Environmental Engineering, Virginia Tech, Blacksburg, May 2002, Available at, <http://scholar.lib.vt.edu/thesis/available/etd-05092002-143014/>
- Neville, A.M., Properties of Concrete, Fourth Edition, John Wiley and Sons, Inc., New York, 1998.
- The Port Authority of New York and New Jersey, Division 3, Section 03301, Portland Cement Concrete, 2000.
- Poston, R., Kesner, K.E., McDonald, J.E., Vaysburd, A.M., and Emmons, P.H., Selecting Durable Repair Materials, Performance Criteria-Laboratory Results, Concrete International, Vol. 22, No. 11, pp. 21-29, November 2000.
- Sakata, K., Prediction of Concrete Creep and Shrinkage, Creep and Shrinkage of Concrete, Proceedings of the Fifth International RILEM Symposium, 1993.
- Suzuki, K., Ohno, Y., and Nakagawa, T., Test Method for Cracking of Concrete Due to Drying Shrinkage, Creep and Shrinkage of Concrete, Proceedings of the Fifth International RILEM Symposium, 1993.
- VDOT, Road and Bridge Specifications, Richmond, 1997.